technical memorandum Daresbury Laboratory

DL/SCI/TM46E

A DETECTION SYSTEM FOR FLUORESCENCE EXAFS AT THE SRS WIGGLER BEAMLINE

by

J.T.M. BAINES, C.D. GARNER, Daresbury Laboratory and Manchester University; S.S. HASNAIN and C. MORRELL, Daresbury Laboratory

FEBRUARY, 1986

Science & Engineering Research Council

Daresbury Laboratory

Daresbury, Warrington WA4 4AD

ABSTRACT

A system for the measurement of fluorescence EXAFS using 6 NaI(Tℓ) scintillation detectors has been commissioned on the Wiggler line of the Daresbury Synchrotron Radiation Source (SRS). Results at the copper and molybdenum K-edges are presented to illustrate the performance of the detectors. The count rate limitations arising from the dead time of the detectors and from the electronics have been investigated. A procedure is described for selecting the optimum thickness of (Z-1) or (Z-2) filter used to reduce the amount of scattered radiation reaching the detectors. Future improvements are discussed.

1. INTRODUCTION

The greater sensitivity of fluorescence detection as compared with absorption measurements has been utilised for some time for the measurement of the Extended X-ray Absorption Fine Structure (EXAFS) of systems containing metals[1-4]. The detection system recently commissioned on the Wiggler line is similar to that in use at the first EXAFS station to be commissioned at the SRS, on line 7[4]. In both systems the signal outputs from a group of NaI(Tℓ) scintillation detectors are summed and fed to a fast multichannel analyser[5] after processing by standard electronics. The Wiggler line is, however, capable of giving intensities an order of magnitude greater than those on line 7, with the result that in some cases (particularly for higher energies and more concentrated samples) the count rate limitations are imposed by the detection system rather than the beam line. Thus an understanding of the effects of dead-time on the EXAFS spectra obtained is important.

2. THE DETECTION SYSTEM

The detection system consists of a frame capable of supporting up to 10 scintillation detectors arranged around the sample. The positions of the detectors are referred to in terms of the angle to the beam direction in the horizontal plane, θ_1, the angle to the horizontal plane, θ_2, and the distance from the sample, r (see fig.1). As yet no focusing optics exist on the Wiggler line, and so the beam is collimated by slits positioned both before and after the monochromator to give a cross-section at the sample of about 10 mm wide by 1-2 mm high. A sample solution is usually contained in

a cell 20 mm wide, 5 mm high and 2-5 mm thick cut out of a plastic or mylar-glass disc with thin mylar windows glued to the front and back faces. The sample cell is mounted at an angle of 45° to the beam as the best quality data is obtained from a detector positioned in the horizontal plane at an angle of 90° to the beam direction. The dependence of the quality of the data obtained on the detector position will be discussed in detail in the following section. Since the edges of the sample cell are strongly absorbing no detectors are mounted in the positions facing them. Only two detectors are mounted behind the sample, i.e. with negative values of θ_1, as here the space available is restricted by the presence of the radiation shielding for another beam line. Thus, at present detectors are mounted in only 6 of the available positions (see fig.1). These positions are listed in table 1. It would be possible to modify the shielding of the adjacent beam line to accommodate further detectors in the future.

TABLE 1

The positions of the detectors in terms of the angles θ_1 and θ_2 and the distance from the sample, r.

Detector	θ_1 (degrees)	θ_2 (degrees)	r (cm)
9	90	0	8
2	90	-45	8
3	90	45	8
4	135	0	8
8	- 90	40	6
10	- 45	0	7

Each detector consists of a cleaved crystal of NaI doped with 1% Tℓ with dimensions 50 mm × 50 mm × 1 mm thick. The crystal is contained in a sealed unit with a Be front window 200 μm thick. A short light guide connects the back of the crystal to a 50 mm diameter photomultiplier tube.

A charge sensitive preamplifier is mounted at the end of each detector. The outputs from the preamplifiers are combined and amplified and fed to two timing filter amplifiers (see fig.2). High frequency pick-

up is removed by integrating the pulses with a time constant of 20 ns. Differentiation with a time constant of 20 ns is used to shorten the pulses. The output from one timing filter amplifier provides the analogue input to the MCA, and the other is discriminated and used to provide the 'convert' pulse. The use of an MCA rather than a scaler allows the pulse height distribution to be displayed. This information can be used to set the level for the threshold of the discriminator.

3. DETECTOR PERFORMANCE

In addition to the fluorescence from the sample, the detectors also receive scattered radiation; both Rayleigh scattered, with a wavelength equal to that of the incident radiation, and Compton scattered, with a wavelength up to 0.05 Å longer. The relative number of fluorescence and scatter counts depends on the concentration of the metal ions giving rise to the fluorescence, the nature of the rest of the sample, the position of the detector and the energy of the incident radiation.

3.1 Count Rates and Fluorescence Fractions

The fluorescence count rate, F, was calculated by subtracting the count rate measured at an energy just below the K-edge being studied, B, where the counts are due purely to background, from that measured just above the edge, where there is a contribution from both fluorescence and scatter (see fig.3). The latter measurement was made at a point at which the amplitude of the EXAFS oscillation was relatively small. The background count rate increases with energy; however, since only a rough comparison of detectors is required, the change in B was ignored.

The results presented here are based on measurements made at the Cu K-edge (at an energy of 9 keV) with a 10 mM solution of $CuSO_4$ as the sample and at the Mo K-edge (20 keV) with a solution of $[NH_4]_6Mo_7O_{24}$ of 10 mM concentration in Mo. The fluorescence, background and total count rates are given in table 2 as ratios to the corresponding count rates for detector 9. The fluorescence fraction, f, which is defined as follows:

$$f = \frac{F}{F + B} \qquad (1)$$

TABLE 2

The performance of each detector at (a) the Cu K-edge and (b) the Mo K-edge. The fluorescence, F_i, background, B_i, and total, $F_i + B_i$, count rates for each detector, i, are given as ratios to the corresponding count rates for detector 9. The fluorescence fraction, f, is given for each detector, along with the figure of merit, X_i, which is given as a ratio to the value for detector 9. The value of the improvement factor, I, quoted for each detector is that obtained when the counts from the detector are combined with those from detector 9.

(a)

Detector i	$\frac{F_i}{F_9}$	$\frac{B_i}{B_9}$	$\frac{F_i+B_i}{F_9+B_9}$	f (%)	$\frac{X_i}{X_9}$	I (%)
9	1	1	1	55	1	-
2	0.47	2.08	1.20	22	0.432	- 0.7
3	0.62	2.67	1.56	22	0.500	1.6
4	1.13	4.43	2.63	24	0.699	12.0
8	0.12	0.45	0.27	25	0.234	- 0.5
10	0.43	4.25	2.17	11	0.293	-19.5

(b)

Detector i	$\frac{F_i}{F_9}$	$\frac{B_i}{B_9}$	$\frac{F_i+B_i}{F_9+B_9}$	f (%)	$\frac{X_i}{X_9}$	I (%)
9	1	1	1	60	1	-
2	0.62	3.14	1.62	23	0.489	0.2
3	0.72	3.49	1.82	24	0.534	2.5
4	1.18	6.44	3.27	22	0.654	5.6
8	0.54	2.13	1.17	28	0.498	4.4
10	1.10	8.08	3.87	10	0.561	- 4.7

is also given for each detector. As the beam is polarised the fluorescence fraction is largest for the detector (9, see table 1) in the horizontal plane at 90° to the beam direction. The angular distribution of the scattered radiation is peaked towards the beam direction, and thus detector 10 has the smallest fluorescence fraction. The detectors positioned normal to the plane of the sample (4 and 10) receive a higher fluorescence count rate than the other detectors on the same side of the sample. This is due to the increased path length through the sample for fluorescence emitted at an angle to the normal. This effect also reduces the count rates for the detectors (2, 3 and 8) out of the horizontal plane. The count rates for these detectors are reduced further by the sample cell which obscures part of the sample. The larger average path length through the sample for fluorescence reaching the detectors behind the sample leads to a reduced count rate for these detectors. Since the sample used at the Cu K-edge was 1 absorption length thick and that used at the Mo K-edge was 0.3 absorption lengths thick, this effect can be seen most clearly with the former sample. The mount for the sample cell obscures part of the sample for detector 2 and so the count rate for this detector is somewhat lower than that for detector 3. With careful design of the sample mount, detectors 2 and 3 would have identical performance; for this reason, in most of the subsequent discussion, results will be given only for detector 3 and the results for detector 2 will be assumed to be the same.

3.2 'Signal-to-noise' Ratio

The quality of the EXAFS spectrum obtained is governed by the ratio of the amplitude of the EXAFS oscillations to the magnitude of the statistical fluctuations in the spectrum. A figure of merit, X, can be defined as follows:

$$X = \frac{F}{\sqrt{(F + B)}} \qquad (2)$$

This quantity is sometimes referred to as the 'signal-to-noise' ratio. The relative values of X for the different detectors are listed in table 2. These values were obtained with a constant incident flux.

The summing amplifiers have the effect of simply summing the counts

from the different detectors (neglecting for the moment the effects of pile-up). In order to determine whether any improvement in the quality of the EXAFS spectra results from adding the signal output from one or more other detectors to that of detector 9, an improvement factor, I, is defined as follows:

$$I = \frac{X_{sum} - X_9}{X_9} \qquad (3)$$

where X_{sum} is the figure of merit obtained from the summed output and X_9 is the figure of merit for detector 9 alone. The values of I obtained when the output from detector 9 is combined with the output from each of the other detectors in turn are also given in table 2. These values depend not only on the value of the figure of merit for the second detector, but also on its count rate. Since the figure of merit for detector 9 is higher than for the other detectors, the addition of counts from a second detector with a relatively high count rate may actually reduce the quality of the resultant EXAFS spectrum. The value of I obtained when the counts from all detectors are summed is given in table 5 along with the resultant increase in count rate. The combination of signals from more than one detector other than by simple summation of counts is discussed in section 6.

4. SIGNAL ENHANCEMENT

To increase the figure of merit and hence improve the quality of the EXAFS spectrum obtained, some method must be found to reduce the background count rate with as small a loss of fluorescence counts as possible. The expression for the figure of merit (eq.2) can be rewritten in terms of the fluorescence fraction (as defined in eq.1) as follows:

$$X = \sqrt{(F.f)} \qquad (4)$$

From this it can be seen that an increase in the fluorescence fraction does not necessarily imply an improvement in the quality of the data.

If the energy resolution of the detectors is sufficiently good, the scattered radiation can be resolved from the lower energy K_α fluorescence

of the sample. If this is not possible, a carefully chosen metal foil placed in front of each detector can be used to absorb preferentially the scattered radiation.

4.1 Energy Resolution

The K_α fluorescence of the sample is produced at an energy 0.93 keV below the absorption edge for Cu and 2.5 keV for Mo. Thus, the energy resolution required to distinguish the sample fluorescence from the elastically scattered radiation is 11% at the Cu K-edge and 13% at the Mo K-edge. The distribution of energies of Compton scsttered photons extends from the energy of the absorption edge to 0.3 keV below it for Cu and 1.5 keV for Mo. Therefore a better resolution is required to resolve the sample fluorescence from the Compton scattered radiation of about 7% at the Cu K-edge and about 5% at the Mo K-edge.

The energy resolution of the NaI(Tl) detectors has been measured to be 35 ± 2% for photons with an energy of 9 keV and 31 ± 3% for 14 keV photons. This energy resolution is not sufficient to resolve the fluorescence completely from the background of scattered photons. To determine whether the energy resolution could still be used to give an improvement in the quality of the EXAFS epectra, X was calculated from measurements made when pulses with a height above some threshold were rejected. Measurements were made at the Cu and Mo K-edges with the upper thrsshold varied from the peak of the pulse height distribution to twice the half width at half maximum above it. The variation in the fluorescence fraction was found to be negligible and in all cases the value of X was reduced as the upper threshold was lowered.

4.2 (Z-1) and (Z-2) Filters

The fluoreecence fraction and, in most cases, the figure of merit can be increased by placing a metal foil in front of each detector. The metal is chosen to have a K-edge below the energy of ths scattered radiation and just above that of the K_α fluorescence of the sample. For a sample containing a 3d metal of atomic number Z, only a metal of foil of atomic number (Z-1) fulfils this requirement. For samples containing a 4d metal, the (Z-2) metal also has a K-edge energy above thst of the K_α fluorescence of the sample. In this case the (Z-2) metal is used in preference to the

(Z-1) metal since the distribution of energies of Compton scattered photons extends below the energy of the (Z-1) K-edge. Such a filter absorbs relatively weakly at the energy of the sample K_α fluorsscence, but strongly absorbs the ecattered radiation. However the K_β fluorescence, which has an energy just below that of the incident radiation and which forms about 20% of the total fluorescence, is also strongly absorbed. A eignificant fraction of the absorbed radiation is re-emitted by the filter as fluorescence.

The change in the figure of merit when a foil of thickness t is placed in front of the detector depends on the absolute number of counts as well as the fluorescence fraction for the detector before the foil is added, f_o. The fractional change in the figure of merit, however, depends only on f_o (provided the amount of multiple Coulomb scattering in the sample is small). It is useful, therefore, to define a quantity Q_t, representing the improvement in the figure of merit due to a foil of thickness t, as follows:

$$Q_t = \frac{X_t - X_o}{X_o} \qquad (5)$$

where X_t and X_o are the values for the figure of merit with and without a foil, respectively. The variation of Q_t with foil thickness is shown in fig.4. Results from measurements at the Cu and Mo K-edges are shown for detectors which have different values for f_o. If f_o is below a critical value, which depends on the nature of the sample and filter, Q_t increases with foil thickness until it reaches a maximum for a thickness t_{max}. The value of t_{max} and the corresponding value of Q_t are given for each detector in table 3. In general the values of these quantities are largest for the detectors with the smallest valuss of f_o. However the values of Q_t measured for detector 8 at the Cu K-edge are much lower than those measured for detector 3 despite the fact that both detectors have similar values of f_o. This is due to multiple Coulomb scattering of the incident radiation as it passes through the sample, which results in scattered photons having an energy below that of the K-edge of the filter. This effect is seen more clearly for the sample used at the Cu K-edge due to the larger thickness of this sample, in terms of absorption lengths.

TABLE 3

The foil thickness, t_{max}, giving the maximum value for the figure of merit and corresponding valus for Q_t.

Detector	Cu K-edge with Ni Foils		Mo K-edge with Zr Foils	
	t_{max}(μm)	Q_t(%)	t_{max}(μm)	Q_t(%)
9	0	0	0	0
3	10	6.2	20	5.0
4	5	7.2	20	1.2
8	0	0	15	5.1
10	5	7.1	35	11.8

4.3 Optimum Foil Thickness

The optimum foil thickness for a deteotor, t_o, is that which gives the maximum value of the figure of merit. For a single detector t_o is equal to t_{max}. However when the counts from several detectors are summed the optimum foil thickness for each detector is, in general, thicker than t_{max}. The optimum foil thickness differs most from t_{max} for the detectors with the highest scatter count rates.

To simplify the determination of the optimum foil thicknesses use is made of the fact that detector 9 has a significantly higher figure of merit than the other detectors. The optimum foil thickness for detector 9 is taken as equal to t_{max}, i.e. the thickness which gives the maximum figure of merit for detector 9 alone. The optimum foil thickness for each of the other detectors is found as that which maximises the figure of merit for that detector summed with detector 9. The variation of the improvement factor, I, with the thicknees of foil placed in front of the second detector is shown for each detector in fig.5. The optimum foil thickness and the corresponding value of I are given for each detector in table 4. Rather than measuring the fluorescence and background count rates with foils in place, these can be calculated from the count rates with no foils, given the attenuation coeffioient of the foil at the fluorescence and background energies and its quantum yield.

Table 4

The optimum foil thickness, t_o, for each detector and the corresponding value for the improvement factor, I. The asterixed values may be up to 5 μm lower than the true value of t_o, the resulting error in I is negligible.

Detector	Cu K-edge with Ni Foils		Mo K-edge with Zr Foils	
	t_o(μm)	I(%)	t_o(μm)	I(%)
3	10	13.2	30*	12.1
4	5	23.5	30*	16.2
8	10	2.1	30*	11.2
10	15*	2.9	50*	15.2

TABLE 5

The fluorescence, F_{sum}, background, B_{sum}, and total, $F_{sum}+B_{sum}$, count rates when all detectors are summed given as a ratio to the count rates for detector 9 alone for the detectors with (i) no foils, (ii) foils thickness t_o and (iii) foils thickness t_{max}. The improvement factor, I, is given for both the unweighted and weighted sum. Results are given for measurements at (a) the Cu K-edge and (b) the Mo K-edge.

(a)

	$\frac{F_{sum}}{F_9}$	$\frac{B_{sum}}{B_9}$	$\frac{F_{sum}+B_{sum}}{F_9+B_9}$	I(%) Unweighted	I(%) Weighted
(i)	3.94	15.47	9.18	29.9	45.9
(ii)	2.76	4.85	3.71	43.1	50.9
(iii)	2.55	3.43	2.95	48.4	50.1

(b)

	$\frac{F_{sum}}{F_9}$	$\frac{B_{sum}}{B_9}$	$\frac{F_{sum}+B_{sum}}{F_9+B_9}$	I(%) Unweighted	I(%) Weighted
(i)	5.27	24.63	13.0	46.4	60.0
(ii)	4.13	9.58	6.67	60.6	65.4
(iii)	3.59	7.11	4.99	60.9	64.1

The value of I for the summed counts from all detectors with optimum thickness foils in place is given in table 5 along with the fluorescence, background and total count rates given as ratios to the values for detector 9 alone. The use of more than one detector significantly improves the quality of EXAFS spectrum that can be obtained for a given incident intensity. A further significant improvement is obtained by the use of filters. The extent of the improvement depends on the concentration of the metal of interest in the sample and to a lesser degree on the energy of the incident radiation. A further benefit of using filters is that a significant reduction in the total count rate per detector is obtained. This is important in the case when the maximum incident intensity that can be used is limited by the count rate capability of the detection system.

5. COUNT RATE LIMITATIONS

There are two sources of loss of efficiency at high count rates; the dead time of the NaI(Tℓ) crystal, and the pulse-pulse resolution of the electronics. The dead time of the scintillator has been measured to be about 250 ns, therefore to obtain better than 90% efficiency the photon rate incident upon each detector must be limited to less than $4.4 \times 10^5\ s^{-1}$. The pulse-pulse resolution of the electronics is also about 250 ns; the resulting loss of counts depends on the distribution of count rates between the different detectors. For a total loss of less than 10% the sum of the count rates incident on each detector must be less than about $4.5 \times 10^5\ s^{-1}$. In order to achieve better than a rough correction for the losses due to these two effects, the count rate from each detector must be known. An additional complication arises from the fact that EXAFS data is occasionally taken when the SRS is operating in single bunch mode. In such a case the incident radiation occurs in bursts separated by a time of 340 ns. Thus each dstector can detect only one photon per bunch, and only one pulse per bunch crossing can be resolved by the electronics. Thus the correction factor for the dead-time is different in this case.

In the chemical interpretation of the spectra obtained, the amplitude of the EXAFS is calibrated as a fraction of the edge height. This amplitude is directly related to the coordination of the atom being studied[6]. An error in the edge height results in an equal fractional error in the coordination numbers determined from the analysis. There will be an error in the calibrated amplitude of the EXAFS if the efficiency of the detection system is different for the pre- and post-edge regions, as is the case when the count rate is dead-time limited. If the efficiency is E_1 in the pre-edge region and E_2 in the EXAFS region ($E_1 > E_2$), then the calibrated amplitude of the EXAFS oscillations will be increased from its value when the efficiency is constant by a factor A given by:

$$A = \left(1 - \frac{E_1 - E_2}{E_2} \cdot \frac{B}{F}\right)^{-1} \qquad (6)$$

The efficiency of the detection system was measured for the distribution of counts obtained from 10 mM solutions of Cu and Mo at their respective K-edges with the optimum thicknesses of foils in place. The efficiencies and corresponding values of A are listed in table 6. For a total count rate in the EXAFS region of $4.1 \times 10^5\ s^{-1}$, A had a value of 1.06; however when the total count rate was increased to $8.6 \times 10^5\ s^{-1}$, A rose to a value of 1.42.

TABLE 6

The factor, A, by which the amplitude of the EXAFS in the background subtracted spectra is increased due to dead-time effects given for two different examples. The count rates below and above the K-edge of the sample B, and F+B respectively, are given along with the corresponding values for the detection efficiencies, E_1 and E_2, respectively.

B (s^{-1})	F+B (s^{-1})	E_1(%)	E_2(%)	A
209 877	406 385	95	90	1.06
591 024	858 979	85	75	1.42

If, when the outputs from all detectors are summed, the count rate leads to an unacceptable error in the amplitude of the EXAFS, the total count rate can be reduced by reducing the incident intensity, reducing the number of detectors, or by increasing the thickness of the foils. It is clear from table 5 that it is better to take data with detector 9 alone

than to use all detectors with reduced incident intensity. This is due to the higher value of the figure of merit for detector 9. If the count rate is too high with detector 9 alone, then it is better to increase the foil thickness rather than to reduce the incident intensity as the foil reduces the count rate due to background more than that due to fluorescence. However, if data is taken with a single detector, it would be possible to correct for the loss of counts due to dead-time when the data is analysed.

6. FUTURE DEVELOPMENTS

The main count rate limitation results from the pulse-pulse resolution of the electronics. This reduces the maximum incident count rate that can be used whilst maintaining an overall efficiency of greater than 90% from the limit of $4.4 \times 10^5\ s^{-1}$ per detector imposed by the scintillator dead-time, to about $4.5 \times 10^5\ s^{-1}$ for all detectors. If data is taken with incident count rates greater than this, the difference in detection efficiency below and above the K-edge of the sample can result in a significant error in the amplitude of the EXAFS in the background subtracted spectrum.

If each detector were to be connected to a separate amplifier, discriminator and scaler, the efficiency of the detection system would be governed predominantly by the dead-time of the NaI(Tl) scintillators. Thus data could be taken with incident count rates of up to $4.4 \times 10^5\ s^{-1}$ per detector without significant errors in the EXAFS amplitude. Furthermore, with such a system it would be possible to correct the number of counts from each detector for losses due to dead-time. This would enable data to be taken with incident count rates of up to about $10^6\ s^{-1}$ per detector without introducing errors in the EXAFS amplitude. There would, however, be a reduction in detection efficiency at high count rates, accompanied by a reduction in pulse height and energy resolution. The MCA would still be used before data collection to set the discriminator threshold so as to remove counts due to electronic noise. Such a readout system is currently being tested.

An additional advantage of having a separate scaler for each detector is that it allows the number of counts from each detector to be combined

other than by simply summing. If, instead, the number of counts from each detector were weighted before summing, then a further improvement in the quality of the EXAFS spectrum could be obtained by a suitable choice of the weights. The figure of merit for the summed detectors is again defined as the ratio of the total number of fluorescence counts to the statistical error in the total number of fluorescence and background counts; in this case, however, the totals are the weighted sums. The figure of merit is given, in this case, by the following expression:

$$X_{sum} = \frac{\sum_i w_i F_i}{\sqrt{\sum_i w_i^2 (F_i + B_i)}} \qquad (7)$$

where F_i and B_i are the fluorescence and background counts for detector i and w_i is the weight. If the value of f_o is chosen as the weight for each detector, then the value of X_{sum} is given by the sum in quadrature of the values of X for each detector. Thus the optimum foil thickness for each detector is equal to t_{max} and the inclusion of another detector always improves the quality of the EXAFS spectrum.

The values for I obtained using a weighted sum are given in table 5 alongside the values obtained with a simple sum. Values are given both for the detectors without foils and with foils of thickness t_{max}. If no foils are used, then the quality of the EXAFS spectrum is significantly improved by performing a weighted sum. If foils are used, however, the value of I is only slightly larger for the weighted case than for the unweighted case. The increase in I resulting from the use of foils is relatively small when a weighted summation is performed; however the total count rate is considerably reduced by the use of foils.

The selectivity with which the metal foil attenuates the scatter rather than the fluorescence is reduced considerably by the fluorescence of the foil which is stimulated by the scattered radiation. Curves of Q_t as a function of foil thickness are shown in fig.6 calculated using different values of f_o. Curves calculated both taking filter fluorescence into account and ignoring it are shown. The greatest reduction in the value of Q_t due to filter fluorescence occurs for the detectors with the smallest

fluorescence fractions. The quality of the EXAFS spectra could, therefore, be improved significantly if the amount of filter fluorescence reaching the detector could be reduced. Such a reduction can be achieved by the use of collimator slit assemblies[7]. Some assemblies of horizontal collimator slits have been constructed (see fig.7); the extended horizontal profile of the beam prevents vertical collimation. These assemblies will absorb 90% of filter fluorescence whilst, if properly aligned, resulting in only about a 15% loss of sample fluorescence. The stand which supports the detectors is currently being modified to allow the collimators to be aligned accurately with the sample and then held rigidly in position.

Due to the dead-time of the NaI(Tℓ) crystal, its detection efficiency is reduced to 80% at an incident count rate of 10^6 s^{-1}. At this count rate there is also a significant loss of energy resolution and pulse height. The count rate incident upon each detector could be reduced by increasing the distance of the detectors from the sample. However, as an increased number of detectors would be required to cover the same solid angle, the fraction of this solid angle taken up by the inactive edges of the detectors would be increased. Also, at low energies, there would be a loss of counts due to absorption by the air. Alternatively higher detection efficiency at high count rates could be obtained by replacing the NaI(Tℓ) crystal with a plastic scintillator. A detector with a 50 mm cube of NE102 plastic scintillator is currently being tested. This scintillator has a dead-time of only 2.5 ns. A scintillator of this thickness will absorb 98% of photons with an energy of 15 keV, and 90% of 20 keV photons. An EXAFS spectrum obtained with this detector at the Cu K-edge is shown in fig.8. A spectrum obtained with a NaI(Tℓ) detector is shown for comparison. Both spectra were taken with the same incident intensity. In both cases the detectors were in the horizontal plane at 90° to the beam direction. The background count rate was higher for the plastic scintillator due to radiation striking the side of the scintillator block. This background could be reduced by shielding the sides of the block.

Plastic scintillators have extremely poor energy resolution. An energy resolution at least as good as that of the NaI(Tℓ) detectors can be obtained using a multiwire proportional gas chamber[8-12]. A detector of this type is capable of count rates of up to about 10^6 s^{-1} per wire with

less than a 5% dead-time loss[12]. In order to achieve these high count rates it is necessary to minimise the distance between the anode and cathode wire planes. However to achieve high detection efficiency a large thickness of gas is required. The detection efficiency is limited to a maximum of 89% by the fluorescence yield of the gas. An active thickness of 10 cm of Xe at atmospheric pressure would give a detection efficiency of 83% for photons with an energy of 15 keV and 62% for 20 keV photons. If the chamber were pressurised to 2 atm. the efficiencies at these two energies would be increased to 89% and 81%, respectively. The two requirements of high detection efficiency and high count rate capability can be simultaneously satisfied either by having a number of alternate closely spaced planes of cathode and anode wires or by having a thick conversion region separated from a thin amplification region by a grid (see fig.9). The former solution has the advantage of smaller drift distances but with greater complexity. A chamber with removable wire planes has been construoted and will be tested in both of the configurations described.

7. CONCLUSION

Good quality EXAFS spectra have been obtained at the Cu and Mo K-edges with the fluorescence detection system commissioned on the Wiggler line. However, it was not possible to utilise the full intensity available owing to the pulse-pulse resolution of the electronics and the dead-time of the detectors. To correct for these effects the count rates from the individual detectors must be recorded. As this is not done at present, the total incident count rate for all detectors must be limited to less than 4.5×10^5 s^{-1} to avoid significant errors in the amplitude of the EXAFS in the background subtracted spectra. With each detector connected to a separate amplifier, discriminator and scaler, the incident count rate could be increased to 4.4×10^5 s^{-1} per detector without significant dead-time effects. With such a system it would be possible to apply a correction for the loss of counts due to the dead-time of the detectors, and thus enable data to be taken with incident count rates of up to about 10^6 s^{-1} per detector without introducing errors in the EXAFS amplitude, but with reduced detection efficiency. The count rate incident upon each detector could be reduced by increasing their distance from the sample. This would,

however, lead to a reduced efficiency at low energies due to absorption by the air. Greater efficiency at high count rates, and a count rate capability of greater than 10^6 s^{-1} per detector could be achieved by replacing the NaI(Tl) scintillators by plastic scintillators or by multiwire proportional gas chambers. However, plastic scintillators have poorer energy resolution than NaI(Tl), whilst a multiwire detector has a maximum detection efficiency of 89%, which is lower than that of the NaI(Tl) scintillators for count rates less than 5×10^5 s^{-1} per detector. Count rates in excess of 10^6 s^{-1} per detector are not available at present, but should become possible if beam focusing optics are installed on the Wiggler line.

The use of (Z-1) or (Z-2) foils placed in front of the detectors significantly improves the quality of the spectra obtained. However, the extent of this improvement is severely limited by the fluorescence of the filter. The amount of filter fluorescence reaching the detector could be greatly reduced by a collimator slit assembly placed between the foil and the detector. However, the slit assembly must be carefully aligned with the sample to minimise the loss of sample fluorescence. A further small improvement in the data could be obtained by performing a weighted summation of the counts, using a weight proportional to the fluorescence fraction for each detector.

ACKNOWLEDGEMENTS

We would like to thank the Science and Engineering Research Council for funding this research, and for the provision of the facilities of the Daresbury Laboratory.

REFERENCES

1. J. Jaklevic, J.A. Kirby, M.P. Klein, A.S. Robertson, G.S. Brown and P. Eisenberger, Solid State Commun., 23 (1977) 679.

2. J.C. Phillips, J. Phys. E: Sci. Instrum., 14 (1981) 1425.

3. S.P. Cramer and R.A. Scott, Rev. Sci. Instrum., 52 (1981) 395.

4. S.S. Hasnain, P.D. Quinn, G.P. Diakun, E.M. Wardell and C.D. Garner, J. Phys. E: Sci. Instrum., 17 (1984) 40.

5. A. Berry, M. Przybylski and I. Sumner, Nucl. Instrum. Meth., 201 (1982) 241.

6. P.A. Lee and J.B. Pendry, Phys. Rev., B11 (1975) 2795.

7. E.A. Stern and S.M. Heald, Nucl. Instrum. Meth., 172 (1980) 397.

8. G. Charpak, D. Rahm and H. Steiner, Nucl. Instrum. Meth., 80 (1970) 13.

9. G. Charpak, D. Demierre, R. Kahn, J.C. Santiard and F. Sauli, Nucl. Instrum. Meth., 141 (1977) 449.

10. A.C. Thompson, Nucl. Instrum. Meth., 195 (1982) 303.

11. G.C. Smith, Nucl. Instrum. Meth., 222 (1984) 230.

12. R. Boie et al., Nucl. Instrum. Meth., 201 (1982) 93.

FIGURE CAPTIONS

Fig.1 The geometrical arrangement of detectors.

Fig.2 The electronics for the fluorescence detection system.

Fig.3 The contribution of background, B, and fluorescence, F, to the EXAFS spectrum.

Fig.4 The variation of Q_t with foil thickness for detectors 9 ( ), 3 ( ), 4 ( ), 8 ( ) and 10 ( ) measured (a) at the Cu K-edge and (b) at the Mo K-edge. The errors shown are purely statistical.

Fig.5 The variation of the improvement factor, I, with foil thickness for detectors 3 ( ), 4 ( ), 8 ( ) and 10 ( ) measured (a) at the Cu K-edge and (b) at the Mo K-edge. The errors shown are purely statistical.

Fig.6 The variation of Q_t with foil thickness for detectors with different values for f_o (a) at the Cu K-edge and (b) at the Mo K-edge. Curves were calculated both taking into account the fluorescence of the filter (solid line) and ignoring it (dashed line).

Fig.7 The collimator slit assembly.

Fig.8 A fluorescence EXAFS spectrum measured at the Cu K-edge using (a) a plastic scintillator and (b) a NaI(Tl) scintillator. The incident intensity was the same in both cases. The ordinate gives the energy above the Cu K-edge. The background counts have been subtracted, and the spectra have been normalised so as to have the same edge height.

Fig.9 Two possible designs for a multiwire proportional drift chamber for fluorescence EXAFS measurement, consisting of (a) a single amplification region separated from a large conversion region by a wire grid, and (b) several combined amplification and conversion regions separated by cathode wire planes.

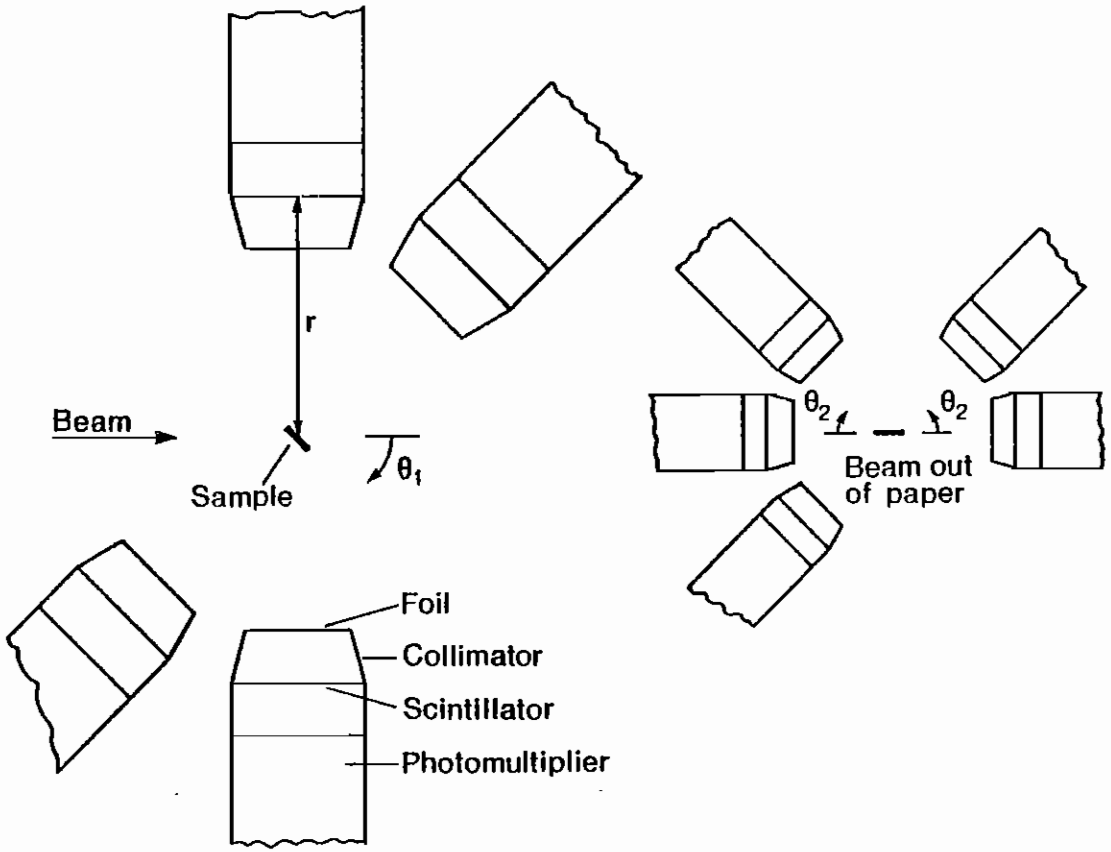

Fig. 1

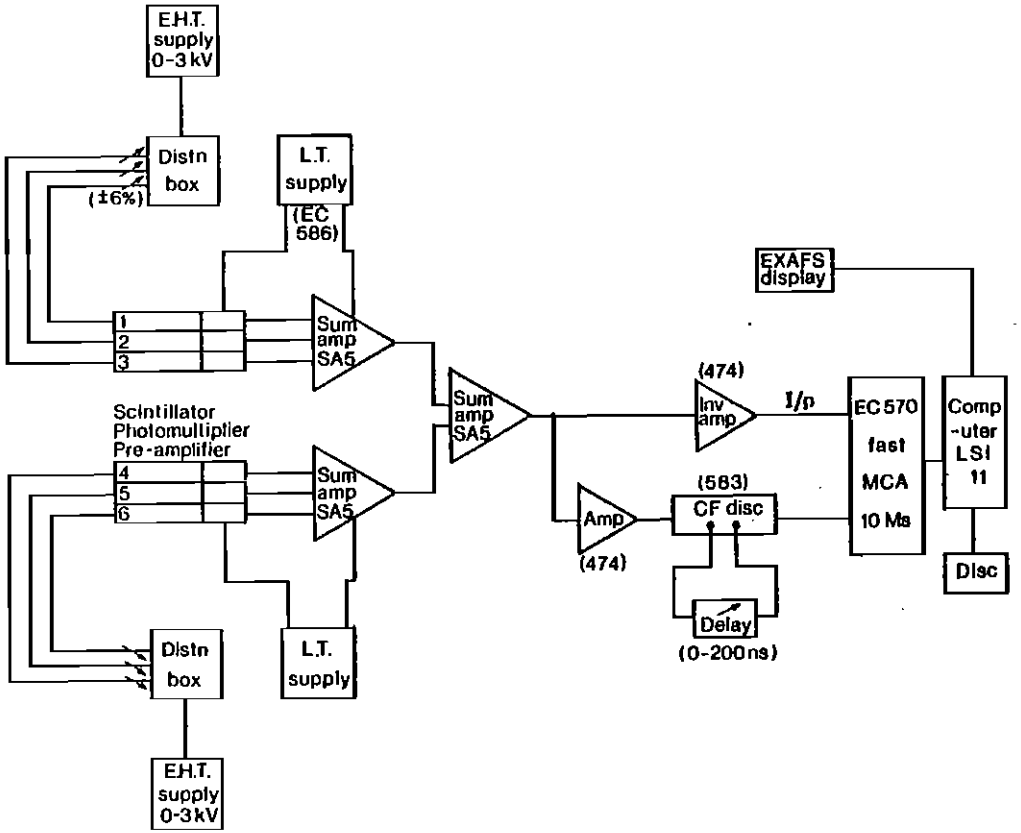
E.H.T. supply 0-3 kV
Distn box
(±6%)
L.T. supply
(EC 586)
1
2
3
Sum amp SA5
Scintillator Photomultiplier Pre-amplifier
4
5
6
Sum amp SA5
Sum amp SA5
(474)
Inv amp
I/p
EC 570 fast MCA 10 Ms
EXAFS display
Comp -uter LSI 11
Disc
Amp
(474)
(583)
CF disc
Delay
(0-200 ns)
Distn box
L.T. supply
E.H.T. supply 0-3 kV

Fig. 2

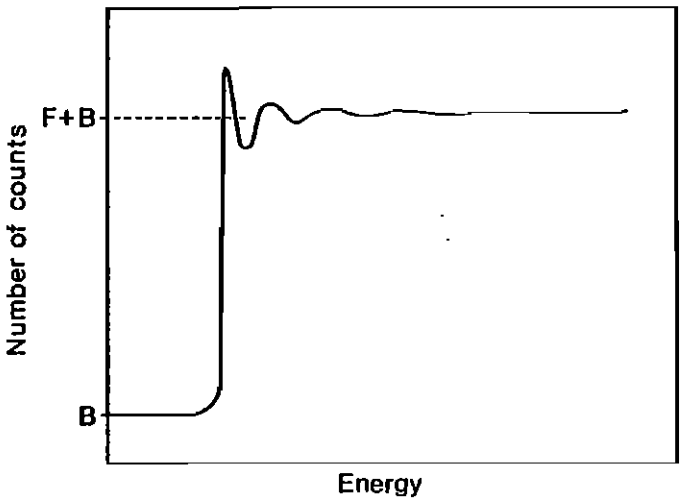
F+B
B
Number of counts
Energy

Fig. 3

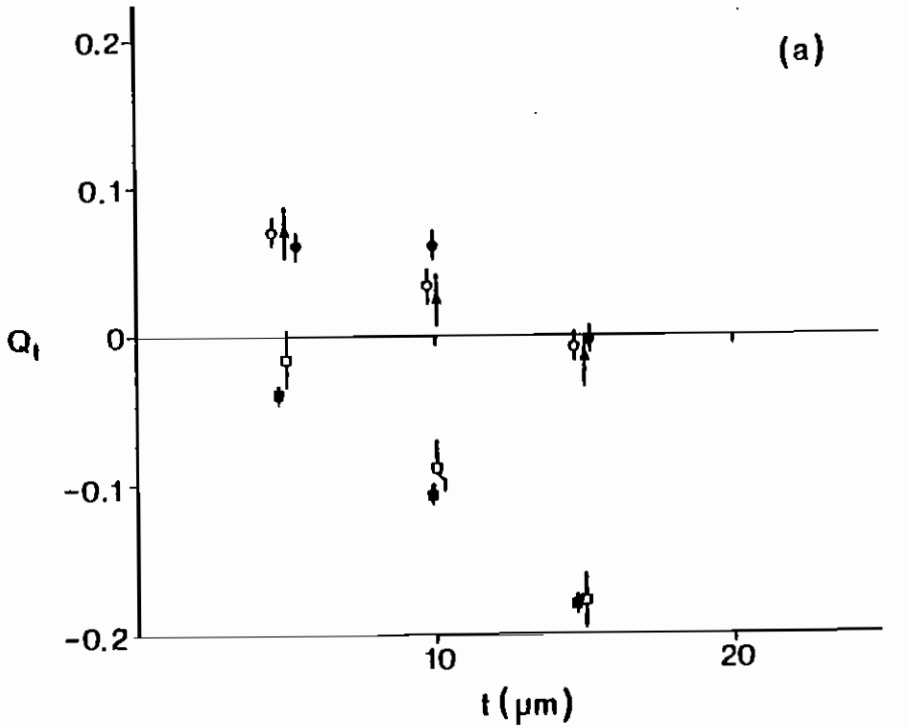
(a)
0.2
0.1
0
-0.1
-0.2
Q_t
10
20
t (μm)

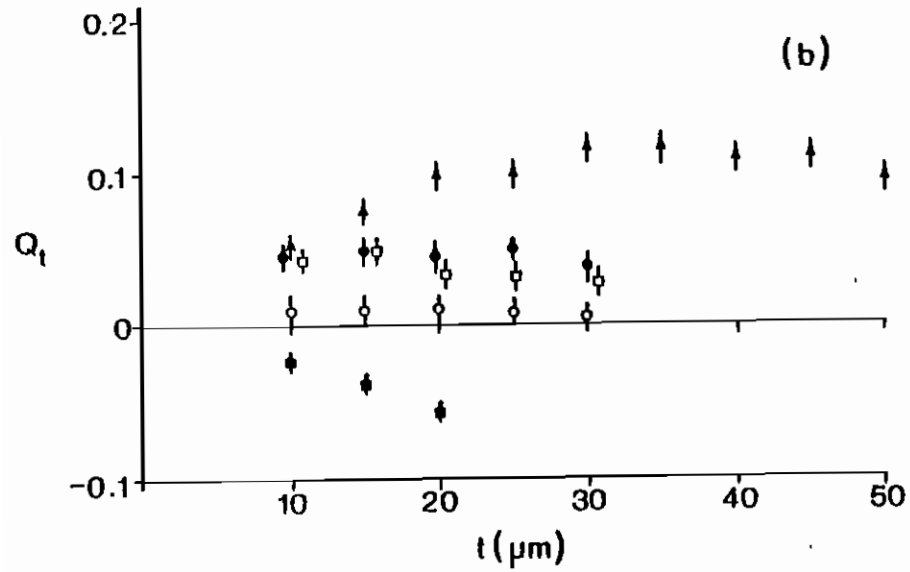
(b)
0.2
0.1
0
-0.1
Q_t
10
20
30
40
50
t (μm)

Fig. 4

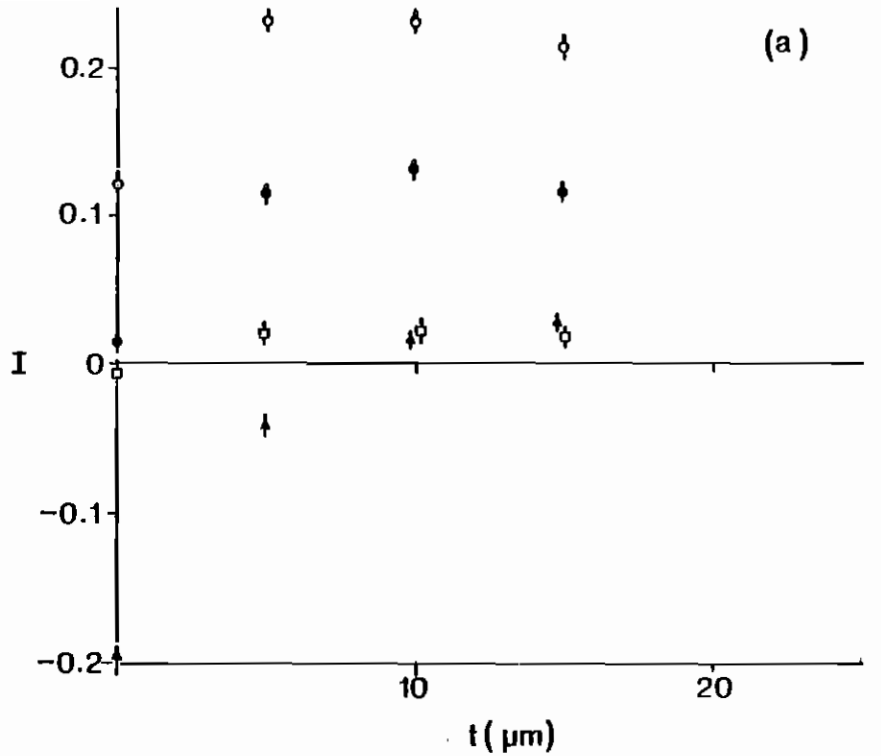
(a)
0.2
0.1
0
-0.1
-0.2
I
10
20
t (μm)

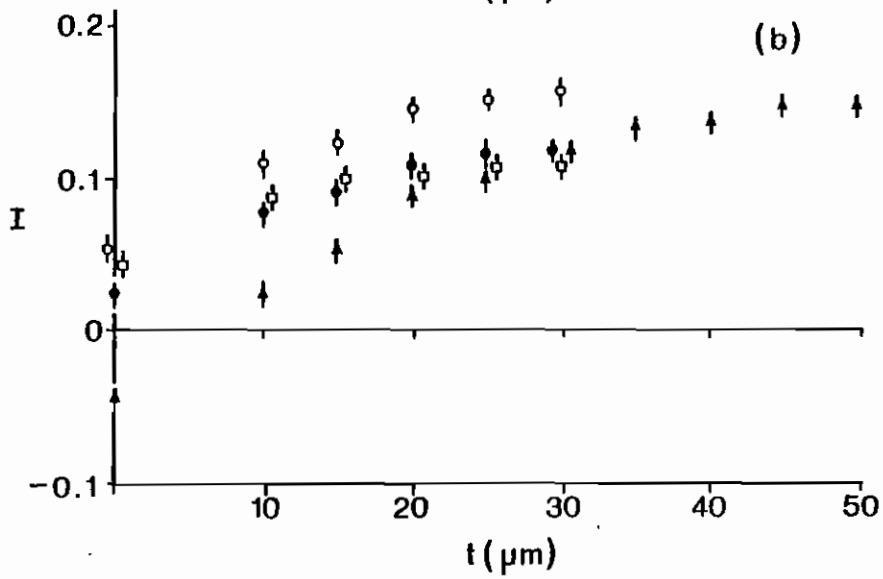
(b)
0.2
0.1
0
-0.1
I
10
20
30
40
50
t (μm)

Fig.5

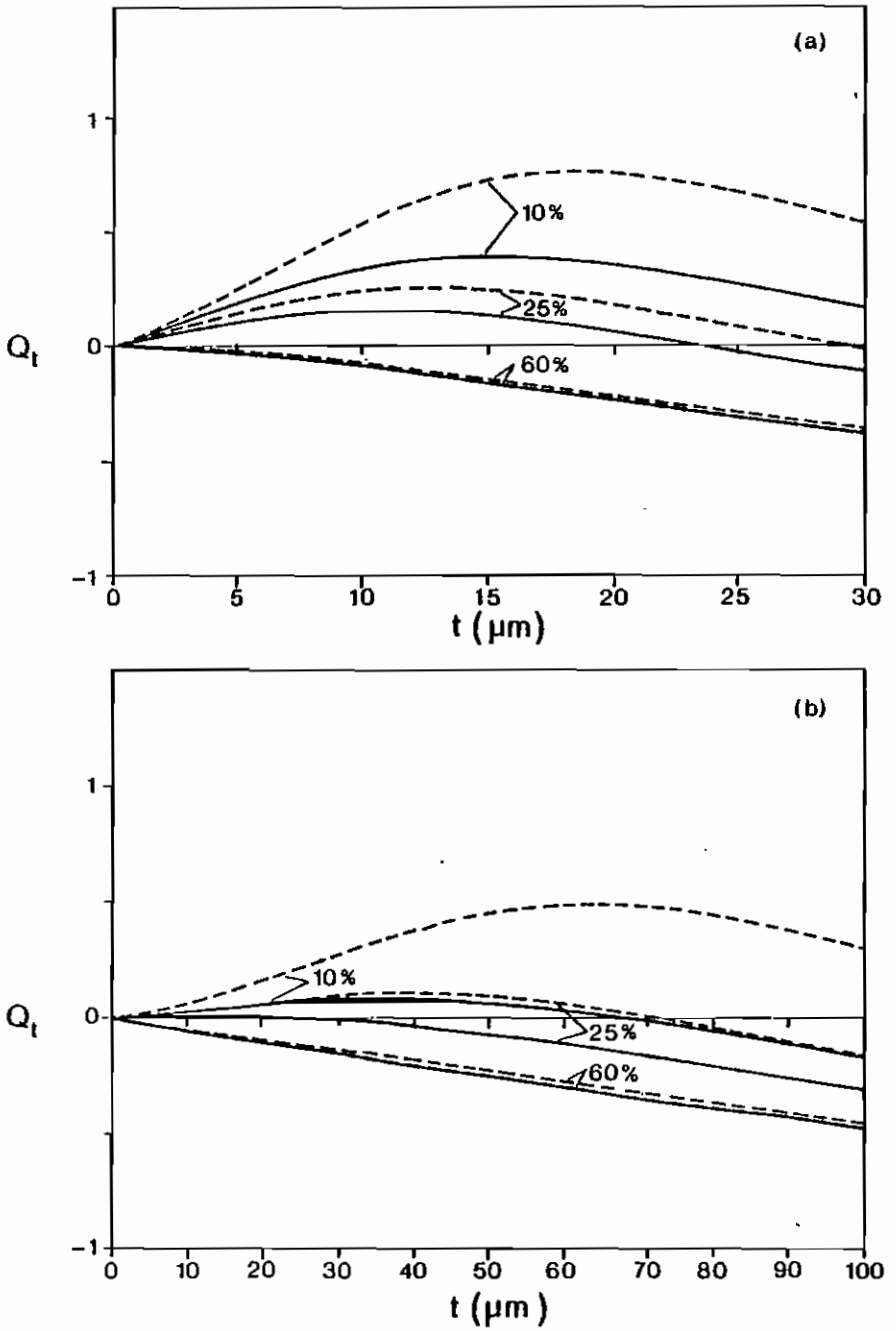
(a)
10%
25%
60%
Q_t
t (μm)
(b)
10%
25%
60%
Q_t
t (μm)

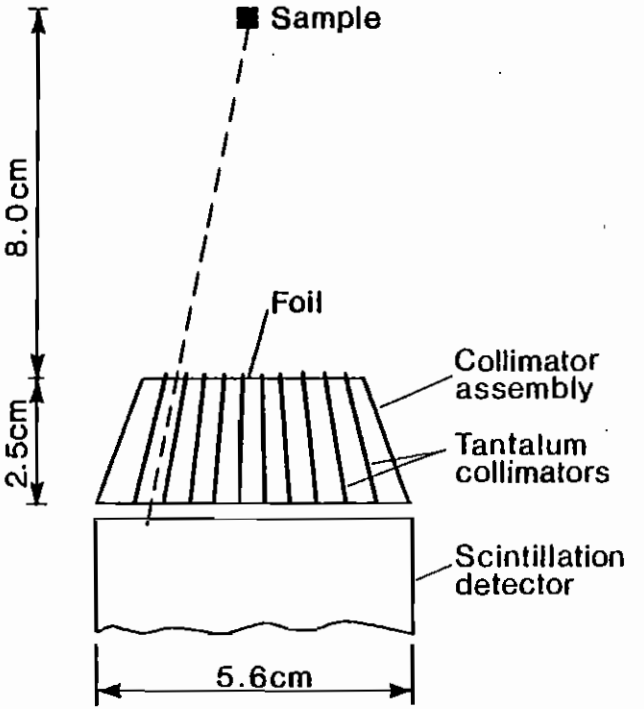
Sample
8.0cm
2.5cm
Foil
Collimator assembly
Tantalum collimators
Scintillation detector
5.6cm

Fig. 7

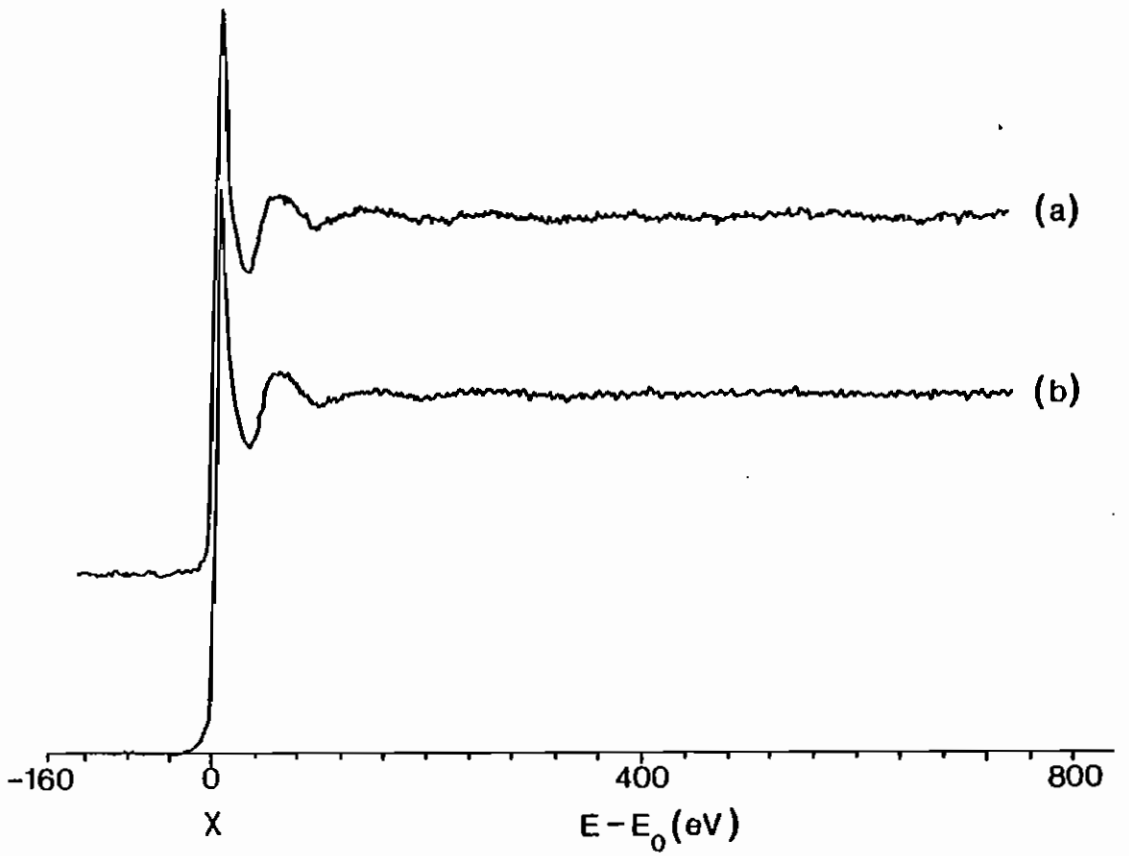
(a)
(b)
-160
0
400
800
X
E - E0 (eV)

Fig. 8

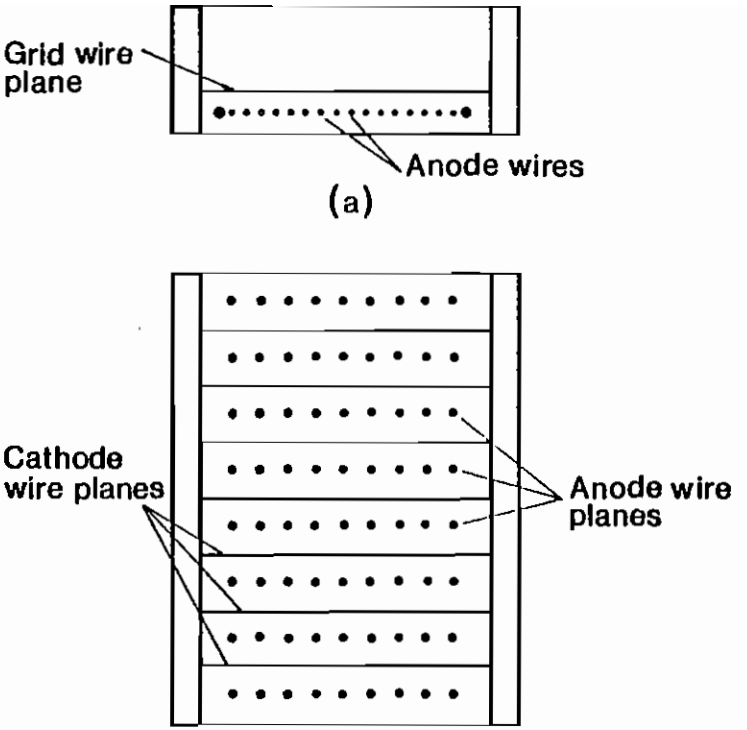
Grid wire plane
Anode wires
(a)
Cathode wire planes
Anode wire planes
(b)

Fig. 9